Supplementary material for "Whole-brain propagating patterns in human resting-state brain activities"

Yusuke Takeda, Nobuo Hiroe, Okito Yamashita

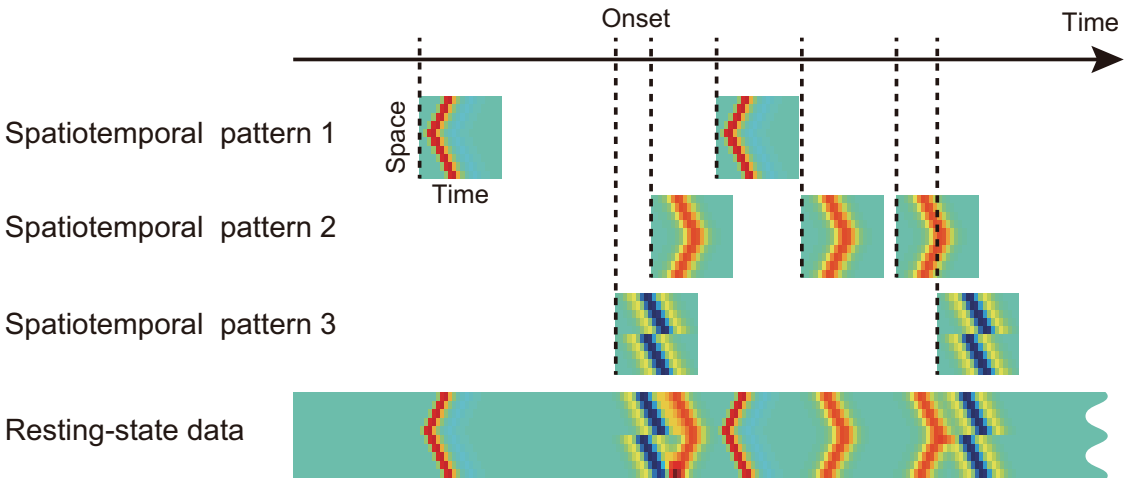

SFigure 1: Assumption of BigSTeP (Takeda et al., 2019). Resting-state data are assumed to contain several unknown spatiotemporal patterns at unknown onsets. Spatiotemporal patterns are defined as observations represented by two-dimensional matrices of space $\times$ time.

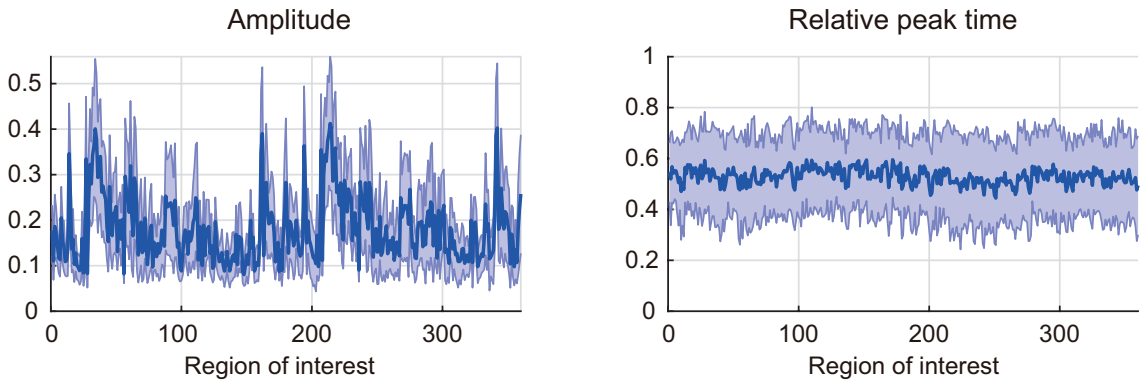

SFigure 2: Variability of amplitudes and relative peak times in spatiotemporal patterns across subjects. Amplitude was calculated for each vertex by averaging pattern's absolute values across times. Relative peak time was defined for each vertex as time when pattern exhibited maximum amplitude across times divided by pattern's length. Amplitudes and relative peak times were averaged within each region of interest (ROI), defined by HCP-MMP1.0 atlas (Glasser et al., 2016). Lines and areas represent their means and standard deviations across patterns and subjects.

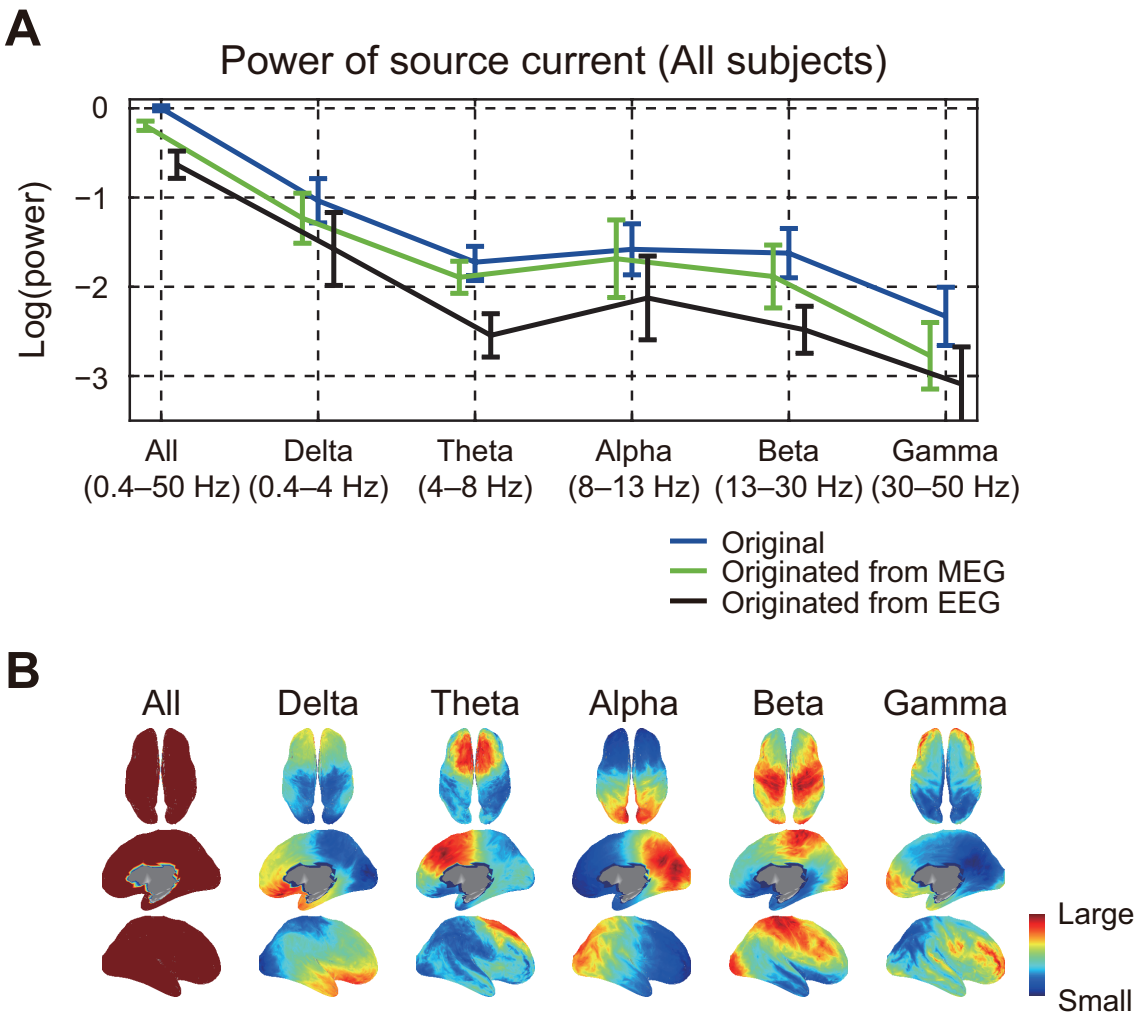

SFigure 3: Powers of source currents in delta, theta, alpha, beta, and gamma bands. They were calculated by an identical procedure as that used for decomposing spatiotemporal patterns into these frequency components (Fig. 3). First, we decomposed the preprocessed MEG and EEG data into these bands using FIR filters. Then we converted the filtered MEG and EEG data into source currents by applying the inverse filter and the normalization used in the source current estimation. Finally, we calculated the powers of the decomposed source currents. (**A**) Power spectrum. Powers were averaged across times, vertices, and subjects. Error bars represent their SDs across subjects. (**B**) Spatial distribution of powers in each frequency band. Powers were averaged across times, patterns, and subjects. For each band, powers over 0.1 of their maximum value are shown. These distributions are consistent with previous MEG study (Niso et al., 2019), suggesting the validity of source current estimation.

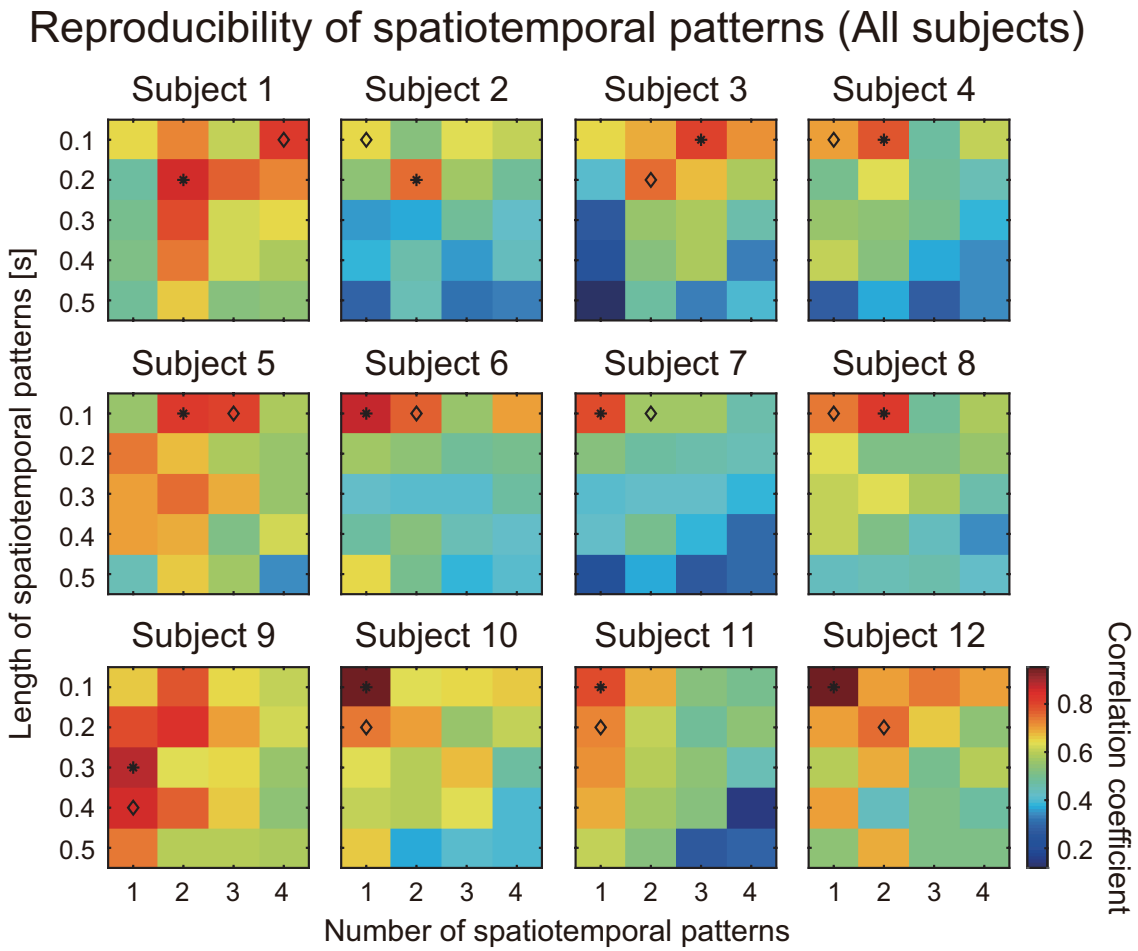

SFigure 4: Reproducibility of spatiotemporal patterns for each pair of hyperparameters: number and length of spatiotemporal patterns. Correlation coefficients of estimated spatiotemporal patterns between two runs are shown for all subjects. For each subject, parameter pairs which exhibited first and second highest correlation coefficients are indicated by asterisk and diamond, respectively.

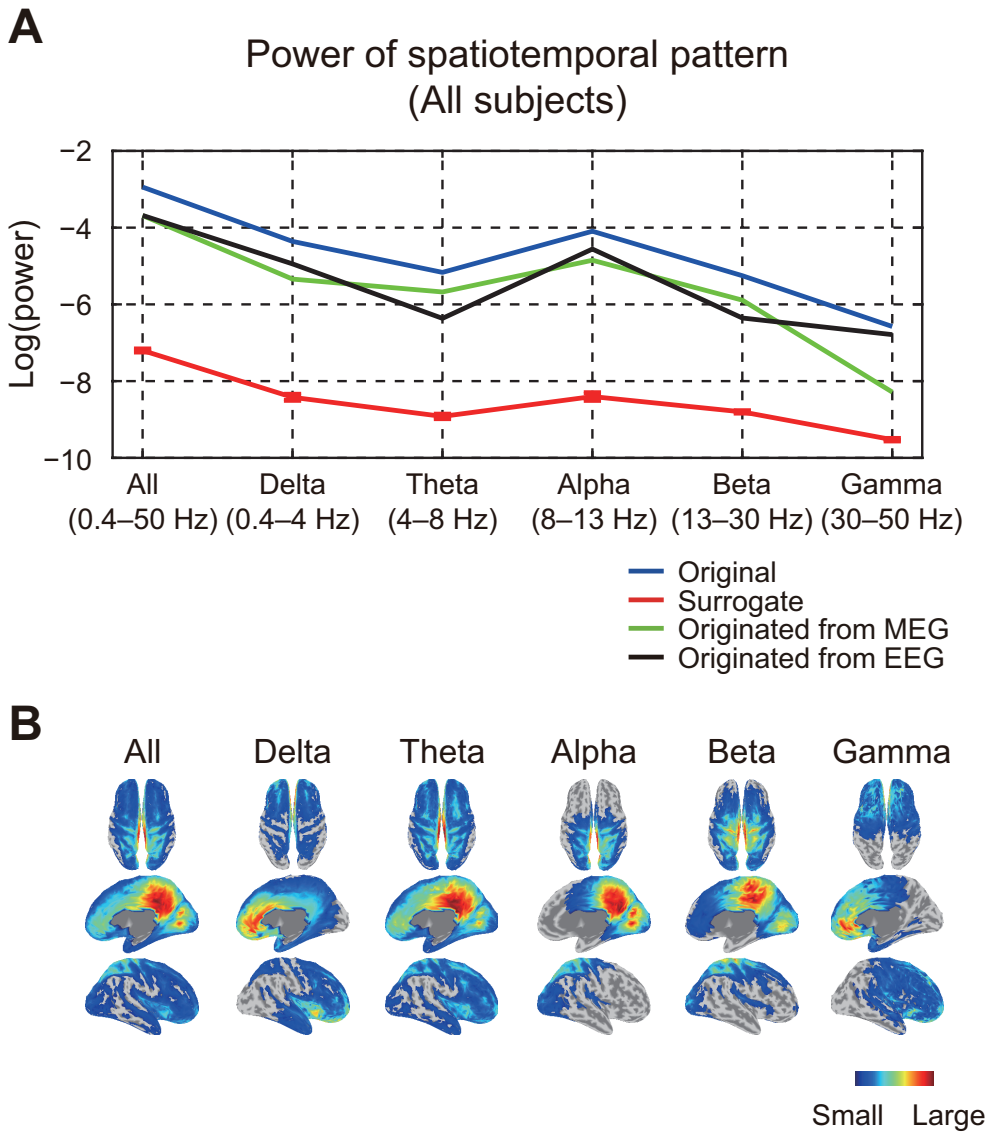

SFigure 5: Temporal frequency of spatiotemporal patterns obtained by hyperparameters that exhibited second highest reproducibility of spatiotemporal patterns (diamonds in SFig. 4). (**A**) Power of spatiotemporal patterns in each frequency component. Powers averaged across times, vertices, patterns, and subjects are shown. Error bars of red line represent SDs of surrogate powers across 1,000 repeats. (**B**) Spatial distribution of spatiotemporal patterns' powers in each frequency component. Powers were averaged across times, patterns, and subjects. For each frequency component, powers over 0.1 of their maximum value are shown.

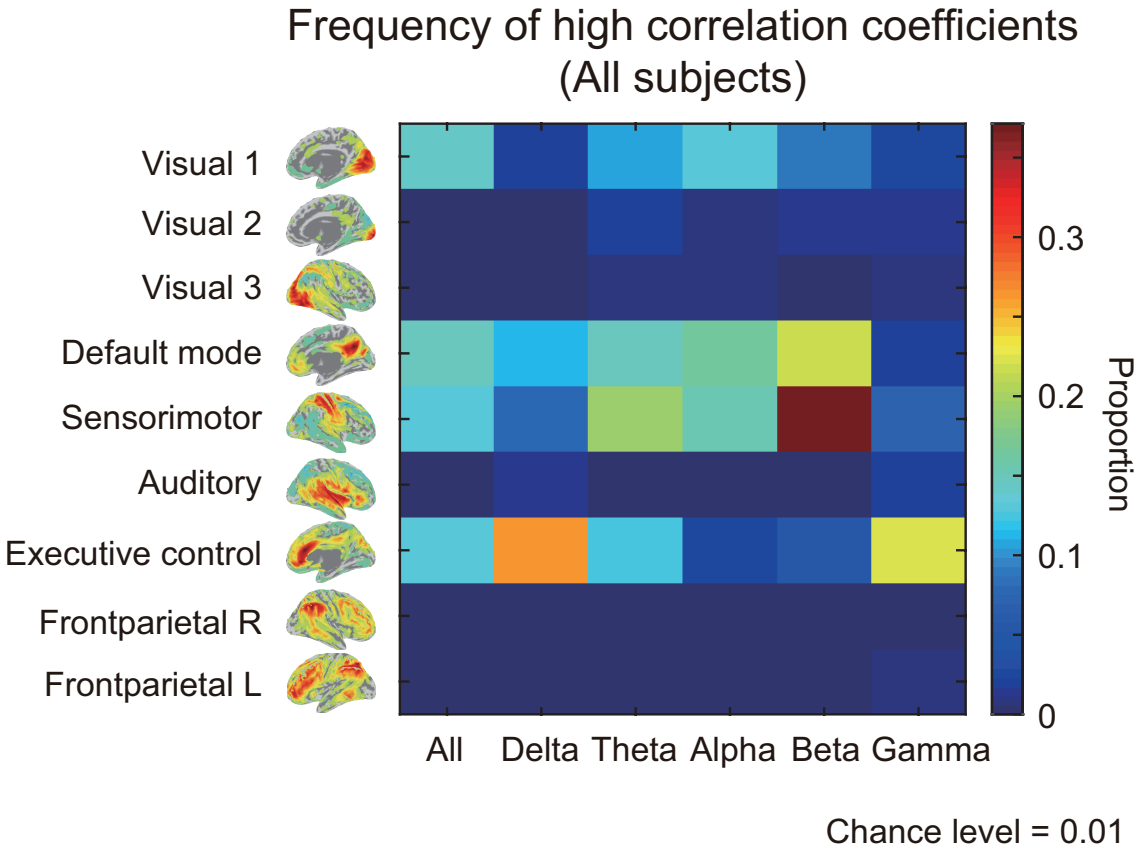

SFigure 6: Similarity between spatiotemporal patterns and fMRI-RSNs obtained by hyperparameters that exhibited second highest reproducibility of spatiotemporal patterns (diamonds in SFig. 4). Proportions of high correlation coefficients ($p < 0.01$) among all times, patterns, and subjects are shown. Chance level was 0.01.

References

Glasser, M.F., Coalson, T.S., Robinson, E.C., Hacker, C.D., Harwell, J., Yacoub, E., Ugurbil, K., Andersson, J., Beckmann, C.F., Jenkinson, M., Smith, S.M., Van Essen, D.C., 2016. A multi-modal parcellation of human cerebral cortex. Nature 536, 171–178. https://doi.org/10.1038/nature18933.

Niso, G., Tadel, F., Bock, E., Cousineau, M., Santos, A., Baillet, S., 2019. Brainstorm pipeline analysis of resting-state data from the open MEG archive. Front. Neurosci. 13, 284. https://doi.org/10.3389/fnins.2019.00284.

Takeda, Y., Itahashi, T., Sato, M., Yamashita, O., 2019. Estimating repetitive spatiotemporal patterns from many subjects' resting-state fMRIs. Neuroimage 203, 116182. https://doi.org/10.1016/j.neuroimage.2019.116182.